Application of Permeability-Limited Physiologically-Based Pharmacokinetic Models: Part II - Prediction of P-Glycoprotein Mediated Drug–Drug Interactions with Digoxin

SIBYLLE NEUHOFF,[1] KAREN ROWLAND YEO,[1] ZOE BARTER,[1] MASOUD JAMEI,[1] DAVID B. TURNER,[1] AMIN ROSTAMI-HODJEGAN[1,2]

[1]Simcyp Limited, Blades Enterprise Centre, Sheffield S2 4SU, UK

[2]School of Pharmacy and Pharmaceutical Sciences, Faculty of Medical and Human Sciences, University of Manchester Manchester M13 9PT, UK

Received 18 April 2013; revised 23 April 2013; accepted 25 April 2013

Published online 19 May 2013 in Wiley Online Library (wileyonlinelibrary.com). DOI 10.1002/jps.23607

ABSTRACT: Digoxin is the recommended substrate for assessment of P-glycoprotein (P-gp)-mediated drug–drug interactions (DDIs) *in vivo*. The overall aim of our study was to investigate the inhibitory potential of both verapamil and norverapamil on the P-gp-mediated efflux of digoxin in both gut and liver. Therefore, a physiologically-based pharmacokinetic (PBPK) model for verapamil and its primary metabolite was developed and validated through the recovery of observed clinical plasma concentration data for both moieties and the reported interaction with midazolam, albeit a cytochrome P450 3A4-mediated DDI. The validated inhibitor model was then used in conjunction with the model developed previously for digoxin. The range of values obtained for the 10 trials indicated that increases in area under the plasma concentration-time curve (AUC) profiles and maximum plasma concentration observed (C_{max}) values of digoxin following administration of verapamil were more comparable with *in vivo* observations, when P-gp inhibition by the metabolite, norverapamil, was considered as well. The predicted decrease in AUC and C_{max} values of digoxin following administration of rifampicin because of P-gp induction was 1.57- (range: 1.42–1.77) and 1.62-fold (range: 1.53–1.70), which were reasonably consistent with observed values of 1.4- and 2.2-fold, respectively. This study demonstrates the application of permeability-limited models of absorption and distribution within a PBPK framework together with relevant *in vitro* data on transporters to assess the clinical impact of modulated P-gp-mediated efflux by drugs in development. © 2013 Wiley Periodicals, Inc. and the American Pharmacists Association J Pharm Sci 102:3161–3173, 2013

Keywords: transporter-mediated drug–drug interactions; P-glycoprotein; ABCB1; MDR1; simulation; digoxin; pharmacokinetics; transporter

INTRODUCTION

P-glycoprotein (P-gp) has a broad substrate specificity, similar to that observed for cytochrome P450 3A4 (CYP3A4), and is therefore, susceptible to a range of drug–drug interactions (DDIs) with a variety of substrates and inhibitors.[1] However, few DDIs, that are clinically relevant, can be attributed solely to the inhibition of P-gp-mediated efflux. This is mainly because of the large overlap in structure-activity that has been reported for CYP3A4 and P-gp, that is, many of the known P-gp substrates are also metabolised by CYP3A4 (e.g. quinidine, verapamil and cyclosporine).[2,3] Similarly, there is often significant overlap in the inhibition potential of P-gp and CYP3A4 by some drugs (e.g. cyclosporine, verapamil). Therefore, it may not always be possible to elucidate the primary mechanism of interaction when both CYP3A4 and P-gp are involved.

Digoxin has been identified as a substrate of P-gp and is mainly excreted unchanged via the kidneys.[4,5] Decreases in renal and extra-renal clearance of digoxin have been proposed as mechanisms for the observed increases in serum digoxin concentrations in patients following co-administration of the calcium antagonist verapamil,[6–11] a P-gp inhibitor. In most of

Correspondence to: Sibylle Neuhoff (Telephone: +44-114-292-2325; Fax: +44-114-292-2222; E-mail: S.Neuhoff@simcyp.com)

Journal of Pharmaceutical Sciences, Vol. 102, 3161–3173 (2013)

the reports citing these results, the P-gp inhibitory effect of the main metabolite norverapamil,[12] which is present at high concentrations in the plasma following oral administration of verapamil,[13] was ignored. However, *in vitro* studies indicate that the metabolite is also a potent inhibitor of P-gp.[12] Although the increases in the area under the plasma concentration-time curve (AUC) of digoxin are relatively small (approximately 35%), they have been associated with serious adverse reactions because of the narrow therapeutic window of digoxin.[14,15]

Current draft guidance issued by the US Food and Drug Administration (FDA),[16] provides recommendations based on *in vitro* data for the assessment of P-gp-mediated DDIs and the drug interaction potential for P-gp substrates and inhibitors.[17,18] For inhibitors, a clinical DDI study with digoxin is recommended if the maximum systemic inhibitor concentration [I_1] at steady state relative to inhibitory potency (K_i; or concentration of inhibitor to inhibit 50% of the P-gp activity; IC_{50}) ratio is > 0.1. The use of the gut concentration of the inhibitor [I_2] (dose/250 mL) has been proposed as an alternative, to predict drug interactions that occur during the absorption phase, but using [I_2]/IC_{50} > 10 as the cut-off. Fenner et al.[1] reported that the former approach was associated with a high percentage of false-negatives (41% based on maximum plasma concentration observed (C_{max})) whereas the latter generated a lower number of false-negatives but a much higher proportion of false positives (50% vs. 13%). Comparable results were obtained in the "P-gp IC_{50} working initiative," where 23 industrial laboratories compared their in-house cut-offs as well as overall cut-offs generated in four different *in vitro* systems and for 16 compounds.[19,20] Thus, for assessment of the P-gp-mediated DDI potential of drugs in development, a more robust quantitative approach is required.

The application of a physiologically-based pharmacokinetic model (PBPK) to predict *in vivo* DDIs involving hepatic transporters from *in vitro* data has been described with respect to the co-administration of repaglinide and cyclosporine.[21–23] Similarly, we have also previously described (Neuhoff et al., Part I)[24] an application of a mechanistic PBPK model for digoxin incorporating the permeability-limited liver (PerL) and the advanced dissolution, absorption and metabolism (ADAM) modules that accounts for regional differences in permeability and P-gp-mediated efflux along the intestine.[25] In the current study, we apply the model developed previously to investigate inhibition and induction of the P-gp-mediated efflux of digoxin in both gut and liver, using interactions with verapamil and its primary metabolite norverapamil and rifampicin as examples.

METHODS

The workflow describing the model building and validation processes that was applied for the digoxin PBPK model was reported previously in the companion report (Neuhoff et al., Part I).[24] A description of the sub-models and the sources of information for digoxin were also provided.

Inhibition of P-gp-Mediated Efflux

The developed model in Neuhoff et al., (Part I)[24] forms the basis to assess the impact of the inhibitor, verapamil, on the PK of digoxin. Assuming that a Michaelis–Menten equation adequately describes cellular uptake or efflux of drug then J_{max} (maximum flux in pmol/min/million hepatocytes or pmol/min/cm^2 of apical intestinal surface area) and K_m (Michaelis—Menten constant in μM) are required to determine $CL_{int,T}$ (transport clearance in μL/min/million hepatocytes or μL/min/cm^2) as follows:

$$CL_{int,T} = \frac{J_{max}}{K_m + Cu} \quad (1)$$

where Cu is the unbound concentration at the transporter binding site. A model accounting for competitive inhibition was used to simulate the effects of verapamil, its metabolite, norverapamil and/or rifampicin on the hepatic and intestinal efflux of digoxin.

Within the ADAM model the concentration of substrate (or inhibitor) at the binding site of P-gp is currently assumed to be the enterocyte concentration, C_{ent}, in the nth segment.[24] Because it is assumed that only the unbound concentration will have access to the transporter binding site, the enterocyte concentration is corrected for the free fraction in the gut (fu_{gut}). For the minimal PBPK model, because the enterocyte concentration is not available, the unbound portal vein concentration is used as a surrogate for the inhibitor.

For the PerL model, the relevant concentrations of both substrate and inhibitor for the canalicular efflux model and hepatic enzyme metabolism are the unbound (unionised and ionised) concentrations in the intracellular water of the liver ($Cu_{IW,Liver}$; Eq. 2).

$$Cu_{IW,liver} = \frac{f_{IW} \times C_{IW,Liver}}{\left(f_{IW} + \frac{Pf_{NL} + (0.3P + 0.7)f_{NP} + Ka_{AP}(AP^-)_{Liver}\alpha}{1+\alpha}\right)} \quad (2)$$

where α for a monoprotic base is: $10^{pKa-pH_{IW}}$ and for other charge types can be defined similarly based on the compound charge type using the Henderson–Hasselbalch equations; f_{IW} is the intracellular water fraction; P is the n-octanol:water partition coefficient

for all tissues except adipose, where it represents the vegetable oil:water partition coefficient. It is assumed that the drug can distribute into the tissue constituents [neutral lipids (NL), neutral phospholipids (NP) and acidic phospholipids (AP)]; f_{NL} and f_{NP} are the liver composition fractions.[26] NPs can be represented by a mixture of 30% NL and 70% water. Ka_{AP} is the association constant of strong bases (pKa > 7.0) for APs [for weak bases (pKa < 7.0), acids and neutral drugs Ka_{AP} is zero].

For rifampicin and norverapamil a minimal PBPK model was used for which $Cu_{IW,Liver}$ is not an available parameter and thus a surrogate is required. Therefore, the unbound emerging concentration from the liver is used as the effective concentration for modelling the inhibition of hepatic canalicular efflux transporters.

$$Iu = \frac{(fu/B:P) \cdot C_{liver}}{(K_p/B:P)} \quad (3)$$

where fu is the fraction unbound in plasma; B:P the blood-to-plasma partition coefficient, K_p is the liver-to-plasma partition coefficient and C_{liver} the liver concentration. The latter is calculated according to the following equation:

$$\frac{C_{liver}}{dt} = \frac{1}{V_{liver}} \left\{ Q_{PV} \cdot C_{PV} + Q_{HA} \cdot C_{sys} - \left[\frac{fu_B \cdot CLu_{int,H}(t)}{(K_p/B:P)} + Q_{PV} + Q_{HA} \right] \cdot C_{liver} \right\} \quad (4)$$

where C_{PV}, C_{sys} and C_{liver} are the concentrations of substrate in the portal vein, systemic circulation and liver, respectively; V_{liver} is the liver volume; Q_{PV} and Q_{HA} are the portal vein and hepatic artery blood flows respectively; fu_B is the unbound fraction in blood (defined by the quotient of fu and B:P) and $CLu_{int,H}(t)$ is the time-variant intrinsic metabolic clearance of the drug in the liver.

The overall inhibitory effect can be modelled using the same approach reported for metabolic interactions[27] (Eq. 5) where *j* represents the inhibitor index of either the parent drug, its metabolites or both:

$$CL_{int,T-inh} = \frac{J_{max}}{K_m \left[1 + \sum_j \frac{(Iu_j)}{Ku_{ji}} \right] + Cu} \quad (5)$$

where $CL_{int,T\text{-}inh}$ is the transporter-mediated intrinsic clearance in the presence of an inhibitor, the "inh" suffix refers to the inhibited value, I_u is the unbound concentration at the binding site of a transporter and K_{ui} is the unbound concentration of inhibitor that supports half maximal inhibition (corrected for non-specific binding). In the case of multiple inhibitors, it is assumed that all inhibitors are acting via the same mechanism (or the overall effect is similar) on each transporter.[27]

Kinetics of Perpetrator Drug

The disposition of verapamil was described by a full PBPK model incorporating both gut and liver permeability-limited models (ADAM and PerL). Enzyme kinetics relating to the formation of the metabolite norverapamil from verapamil via CYP2C8, CYP3A4 and CYP3A5 were assessed.[28,29] Time-dependent inhibition (TDI) of metabolism was also considered for verapamil. The disposition kinetics of rifampicin was described by a lumped minimal PBPK model. The model lumps all organs except the liver—its structure and applications have been described previously.[30] Values of CYP3A4 enzyme turn over (k_{deg}) used for the simulations were 0.019 and 0.030 h^{-1} in the liver and gut, respectively.[31,32]

Data Used for Rifampicin, Verapamil and Norverapamil Simulations

In vitro and pharmacokinetic parameters for verapamil, norverapamil and rifampicin are shown in Tables 1–3, respectively. Where data from more than one source were available for the same parameter, weighted means were calculated based on the number of observations reported. In the absence of kinetic transport data (J_{max}, K_m) for norverapamil a hepatic uptake factor of 2, which is equivalent to the contribution of hepatic uptake to the clearance of verapamil, was applied in the simulations.

P-gp Inhibition Data

P-glycoprotein inhibition data were collated from the literature. Only data obtained using Caco-2 cells and digoxin as the victim drug were selected, to avoid bias from other *in vitro* systems (difference in passive permeation and other transporters). In addition to those recently published by the "P-gp IC_{50} working group," 55 independent values for K_i and/or IC_{50} for verapamil were found in the literature; of these, eight were measured in Caco-2 cell monolayers with digoxin as the substrate. IC_{50} values ranged from 0.1 to 36.2 μM for verapamil (Table 4). To investigate the worst-case scenario, the lowest K_i value calculated from the IC_{50} data was used in all simulations.[33] A single IC_{50}-value of 0.3 μM was found for norverapamil[12] and an IC_{50}-value of 169 μM was reported for rifampicin.

P-gp Induction Data

Data relating to induction of intestinal P-gp by rifampicin were used to investigate the effect of this inducer on the systemic exposure to digoxin. To model the concentration-dependent effect of rifampicin on

Table 1. Final Input Data Used for Verapamil

Parameter	Value	Reference/Comment
Dose (mg)	80 t.i.d.	
MW (g/mol)	454.60	
fu–experimental	0.091	Meta-analysis[47,48]
B:P–experimental	0.705	Ref. 48
log *P*–experimental	3.81	Sangster database;[49]
Absorption		
Absorption model	ADAM	
Compound type	Monoprotic base	
pKa–experimental	8.92	Simcyp library value
Caco-2 (apical pH 7.4/basolateral pH 7.4; 10^{-6} cm/s)	156.6	Refs. 50,51
Reference compound—propranolol	109	Ref. 52
Distribution		
Distribution model	Full PBPK	
V_{ss} (L/kg)–predicted	5.37	Predicted from Rodgers and Rowland method using a K_p scalar of 2.78, see text
V_{ss} (L/kg)–observed	5.37	Meta-analysis[13,53–58]
CL_{iv} (L/h)	55.37	Meta-analysis[13,53–55]—used within the Retrograde model
CL_R (L/h)	2.4	Ref. 59–used within the Retrograde model
Transporter data		
Intestinal efflux		
J_{max} (pmol/min/cm^2)–P-gp	18.4	Assigned based on efflux clearance and K_m
K_{mu} (μM)–P-gp	4.1	Ref. 60
Intestinal P-gp REF for MDCK–MDR1	1.5	Ref. 61
CL_{intT} (μL/min/cm^2)—additional—MRP2	25	Fitted based on evidence in Ref. 51
Intestinal MRP2 REF (user input) 1		
Hepatic efflux (P-gp)		
J_{max} (pmol/min/million hepatocytes)	18.4	Assigned based on efflux clearance and K_m
K_{mu} (μM)	4.1	Ref. 60
Hepatic P-gp REF for MDCK–MDR1	1.125	Scaled according to Caco-2 scalar with Simcyp V12R2
% Reabsorbed	100	Assumed because of the high $P_{eff,man}$ measured[50]
Hepatic uptake (OCTN2 and additional)		
CL_{intT} (μL/min/million hepatocytes)–OCTN2	55	Ref. 62—assuming activity in 1 million hepatocytes equal activity in 1 mg protein of the HEK293-OCTN2 cells
Hepatic OCTN2 REF for HEK293-OCTN2	1	Assumed
CL_{intT} (μL/min/million hepatocytes)—additional	500	Assumed with a REF of 1. Note this could also be combined with the OCTN2, by increasing that REF to (555/55 =) 10.1; however, evidence suggests a second hepatic uptake transporter.
CL_{PD} (mL/min/million hepatocytes)	0.297	Ref. 62—assuming activity in 1 million hepatocytes equal activity in 1 mg protein of the HEK-OCTN2 cells
Metabolism data		Assigned using the Retrograde model (input CL_{iv} and CL_R)
R/S-Norverapamil		
CYP2C8–CL_{int} (μL/min/pmol of isoform)	2.39	fm assigned based on Refs. 28,29
CYP3A4–CL_{int} (μL/min/pmol of isoform)	0.34	fm assigned based on Refs. 28,29
CYP3A5–CL_{int} (μL/min/pmol of isoform)	0.69	fm assigned based on Refs. 28,29
D-617		
CYP2C8–CL_{int} (μL/min/pmol of isoform)	1.70	fm assigned based on Refs. 28,29
CYP3A4–CL_{int} (μL/min/pmol of isoform)	0.37	fm assigned based on Refs. 28,29
CYP3A5–CL_{int} (μL/min/pmol of isoform)	0.45	fm assigned based on Refs. 28,29
D-702 and D-703		
CYP2C8–CL_{int} (μL/min/pmol of isoform)	2.27	fm assigned based on Refs. 28,29
Inhibition data		
K_i–intestinal P-gp (μM)	0.1	Ref. 20
K_i–hepatic P-gp (μM)	0.1	Ref. 20
k_{inact} (h^{-1})–CYP3A4	2	Ref. 31
fu_{mic}–CYP3A4	1	Ref. 31
K_{app} (μM)–CYP3A4	2.21	Ref. 31
k_{inact} (h^{-1})–CYP3A5	1.75	Ref. 31
fu_{mic}–CYP3A5	0.77	Ref. 31
K_{app} (μM)–CYP3A5	5.4	Ref. 31

Absorption: Note that comparable $P_{eff,man}$ values to *in vivo* were predicted using Caco-2 (7.4/7.4; passive), MDCK II or PSA/HBD as input option.

Table 2. Final Input Data Used for Norverapamil

Parameter	Value	Reference/Comment
MW	440.60	
fu - experimental	0.08	Meta-analysis[48,63]
B:P–experimental	0.670	Refs. 48,64
log *P* - predicted	3.665	Advanced Chemistry Development, Inc. (ACD/Labs)
Compound type	Monoprotic base	
pKa–experimental	8.6	Ref. 65
Distribution model	Minimum PBPK	
V_{ss} (L/kg)	5.37	Assumed same as parent
$t_{1/2}$ (h)	6.59	Refs. 13,55,59
CL_{iv} (L/h)	39.52	Calculated as ke (h^{-1}) ×V (L)
CL_R (L/h)	2.37	6% of dose[66]
Metabolism data		Assigned using the Retrograde model (input CL_{iv} and CL_R)
D620		
CYP2C8–CL_{int} (μL/min/pmol of isoform)	2.279	fm assigned based on Ref. 29
CYP3A4–CL_{int} (μL/min/pmol of isoform)	0.395	fm assigned based on Ref. 29
CYP3A5–CL_{int} (μL/min/pmol of isoform)	1.065	fm assigned based on Ref. 29
D-715		
CYP2C8–CL_{int} (μL/min/pmol of isoform)	3.774	fm assigned based on Ref. 29
Active uptake into hepatocytes	2	Corresponding to 18% of clearance
Inhibition data		
K_i–intestinal P-gp (μM)	0.3	Ref. 12
K_i–hepatic P-gp (μM)	0.3	Ref. 12

the induction of P-gp mechanistically, turnover numbers of P-gp are required. As these data are not available, we used an approach that involved application of an intestinal relative expression factor (REF). The REF is the ratio of intestinal transporter abundance in *Jejunum I* (per cm^2 of cylindrical surface area) versus that of the *in vitro* system (per cm^2), where *Jejunum I* represents a segment of the ADAM model.[25] This value can be obtained by comparing relative abundances derived from Western blot studies or by comparison of absolute abundance data from LC–MS/MS studies. The REF can be replaced with a RAF, that is, a relative activity factor, which is considered to be more relevant. However, REF and RAF can be used interchangeably assuming the same activity per transporter molecule *in vivo* and *in vitro*. In the study of Greiner et al., a 3.5-fold increase in *in vivo* P-gp expression was observed following multiple doses of rifampicin [600 mg *quaque die* (q.d.) for 10 days]. Thus, assuming that steady state concentrations had been obtained for rifampicin, a REF of 3.5 was applied to simulations involving rifampicin.

Table 3. Parameter Values used for the Rifampicin Simulations

Parameter	Value	Reference/Comment
Dose (mg)		
MW (g/mol)	823	
log *P*	3.28	AlogPS web site (in 2009)
Compound type	Ampholyte	
pKa	1.7 (acid); 7.9 (base)	
fu	0.15	Ref. 67
B:P	0.9	Ref. 38
fa	1	Assumed
ka (1/h)	0.51	Ref. 68
V_{ss} (L/kg)	0.33	Recalculated using WinNonLin[38]
CL_{po} (L/h)	21.6	Ref. 69
CL_{iv} (L/h)	7	Simcyp library value.
CL_R (L/h)	1.2	Ref. 69
K_i–CYP3A4	10.5	Simcyp library value, corrected for the unbound fraction in the microsomal incubation (fu_{mic})[70]
$IndC_{50}$–CYP3A4/5 (μM)	0.32	Simcyp library value. Fitted based on *in vivo* data.[71,72]
Ind_{max}–CYP3A4/5 (fold)	8	Simcyp library value. Fitted based on *in vivo* data.[71,72]
K_i–intestinal P-gp (μM)	164	Personal communication
K_i–hepatic P-gp (μM)	164	Personal communication
Fold of intestinal P-gp induction	3.5[a]	Ref. 4

[a] Induction after 6 days of 600 mg q.d. rifampicin was measured with a quantitative Western blot.

Table 4. Inhibition Data for Verapamil, Norverapamil and Rifampicin Using Caco-2 Cell Monolayer and Digoxin as Victim Drug

Compound	IC_{50} (μM)	K_i (μM)	Reference/Comment
Verapamil	1.1	1.07[a]	Ref. 12
Verapamil	2.1	2.04[a]	Ref. 73
Verapamil	2.1	2.04[a]	Ref. 74
Verapamil	4	3.89[a]	Ref. 75
Verapamil	10	9.73[a]	Ref. 1
Verapamil	16.8	16.3[a]	Ref. 76
Verapamil	–	8.11	Ref. 77
Verapamil	0.1	0.1[a]	Lowest value from Refs. 19,20
Norverapamil	0.3	0.3[a]	Ref. 12
Rifampicin	169	164[a]	Personal communication

[a]Calculated K_i from IC_{50} value (within the Simcyp Simulator) using the assumptions by Cheng and Prusoff.[33]

Simulations

The models and differential equations described above are components of the algorithms implemented within the Simcyp population-based simulator (Version 12.2; Simcyp Ltd., Sheffield, UK).[34] The program allows facile extrapolation of *in vitro* enzyme kinetic data, in both liver and intestine, to predict pharmacokinetic changes *in vivo* in virtual populations. Genetic, physiological and demographic variables relevant to the prediction of DDIs are generated for each individual using correlated Monte Carlo methods and equations derived from population databases obtained from literature sources.[35]

The Simcyp Simulator (Version 12.2) was used to simulate the time courses of digoxin, verapamil, norverapamil and rifampicin concentrations in plasma. To ensure that the characteristics of the virtual subjects were matched closely to those of the subjects studied *in vivo*, numbers, age range and gender ratios were replicated. Ten separate trials for each replicated clinical study were generated to assess variability across the population. Three sets of DDI simulations were run using either verapamil and norverapamil or rifampicin as perpetrators. To obtain reliable predictions of transporter-mediated DDIs (tDDIs), it is important to ensure that the PBPK model developed for verapamil and its metabolite is able to recover observed plasma concentrations and more importantly, clinical DDIs, including those CYP-mediated, thus demonstrating that the model generates appropriate concentrations in gut and liver for inhibition of both transport and metabolism. Specifically, simulations using the study designs described below were run.

- TDI of CYP3A4-mediated metabolism by verapamil: Ten virtual trials of nine female subjects aged 19–28 years receiving 15 mg midazolam on day 2 at 3:30 pm and five oral dose of 80 mg [*ter in die* (t.i.d.) or "three times a day"] starting on day 1 at 2:30 pm. Thus, midazolam was given 1 h after the 4th dose of verapamil corresponding to the study design reported by Backman et al. (1994).[36] Simulations were performed and compared with observed data for midazolam, verapamil and norverapamil.[13,36]
- Inhibition of P-gp-mediated efflux of digoxin by verapamil and norverapamil: Ten virtual trials of 19 male subjects aged 23–40 years receiving 0.25 mg digoxin [*bis in die* (b.i.d.) or "twice a day"] for 14 days followed by co-administration of 80 mg verapamil (t.i.d.) for another 14 days were generated and the simulated profiles for digoxin and verapamil were compared with those observed by Rodin et al.[37] The morning dose of digoxin was given 30 min after administration of the morning dose of verapamil.
- Induction of P-gp-mediated efflux of digoxin by rifampicin: Ten virtual trials of eight male subjects aged 21–37 years receiving a single oral dose of 1 mg digoxin were generated. In a second simulation, 10 virtual trials of eight male subjects aged 21–37 years receiving 600 mg rifampicin (q.d. or "one a day") on days 1–16 and a single oral dose of 1mg digoxin on day 11 were generated. In the latter simulation, the intestinal REF for P-gp was increased by 3.5-fold based on *in vitro* data reported by Greiner et al.[4] The simulated profiles for digoxin and rifampicin were compared with those observed by Greiner et al.[4] and Loos et al., respectively.[38] Predicted and observed ratios of C_{max} and area under the plasma concentration-time curve ($AUC_{(0-\infty)}$) values for digoxin in the absence and presence of rifampicin were compared.

RESULTS

Prediction of the Midazolam–Verapamil DDI

Predicted and observed[36] mean plasma concentration–time profiles of midazolam after a single oral dose of 0.15 mg in the absence and presence of verapamil (80 mg t.i.d.) were compared for 10 virtual trials (Figs. 1a and 1b). The corresponding simulated concentration–time profiles for verapamil and norverapamil are shown in Figures 1c and 1d, respectively. No data were available for norverapamil to make direct comparisons between observed and predicted profiles. Thus, a profile for norverapamil from a study with comparable dose was used. The change in intestinal and hepatic CYP3A4 and CYP3A5 content as a result of verapamil administration is shown in Figures 1e and 1f, respectively. The predicted mean AUC ratio for midazolam in the presence and absence of

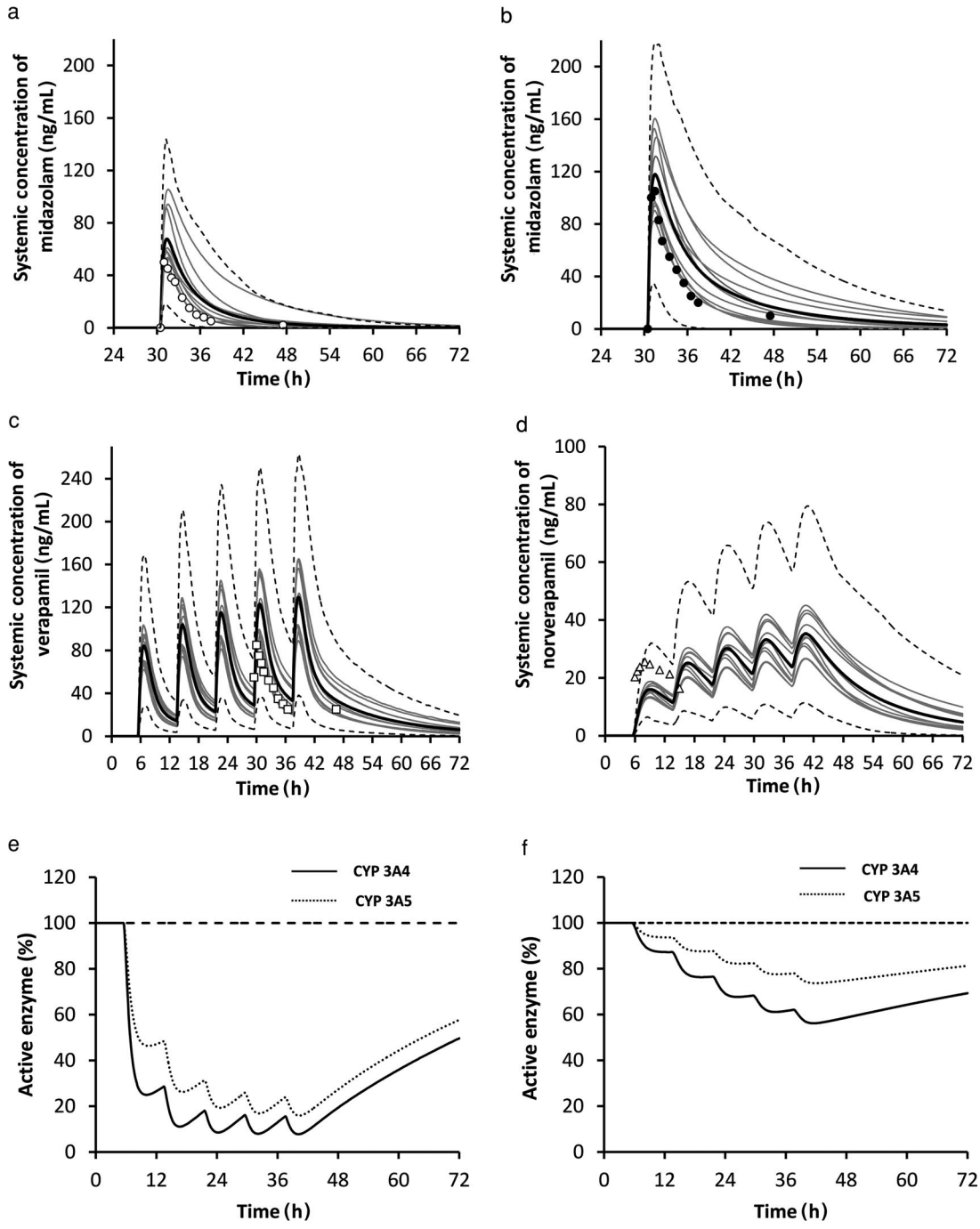

Figure 1. Comparison of observed and predicted plasma midazolam concentration–time profiles after a single 15 mg dose (a) in the absence and (b) presence of verapamil (80 mg t.i.d.) and its major metabolite, norverapamil. Comparison of observed and predicted plasma verapamil (c) and norverapamil (d) concentration–time profiles. Key: The thick lines represent the mean of the simulated population ($n = 90$), the thin lines represent the individual 10 trials and the thin black dashed lines are the 95th and 5th percentile of the confidence interval. Open circles—observed midazolam concentrations when administered alone;[36] closed circles—with co-administration of verapamil;[36] open square—observed verapamil concentrations;[36] open triangle—observed norverapamil concentrations.[13] The changes in gut and hepatic CYP3A4 (dense black line) and CYP3A5 (dotted line) content as a result of verapamil administration are shown in (e) and (f), respectively.

verapamil and its metabolite was 2.74, ranging from 1.87 to 3.51 for the 10 trials. These values were consistent with the observed AUC ratio of 2.9, thus, verifying the validity of the PBPK model for verapamil and its major metabolite norverapamil for assessment of inhibitory potential, albeit with respect to CYP3A4.

Prediction of the Digoxin–Verapamil DDI

Predicted and observed[37] mean plasma concentration–time profiles of digoxin after oral dosing of 0.25 mg (b.i.d.) for 14 days followed by co-administration of verapamil (80 mg, t.i.d.) for an additional 14 days in 10 virtual trials are shown in Figures 2a and 2b, respectively. Simulated mean plasma concentration–time profiles associated with 80 mg verapamil (t.i.d.) during 14 days of dosing are shown in Figure 2c; no data were available for verapamil in the experimental study to make direct comparisons between observed and predicted profiles. Therefore, profiles of verapamil from comparable dose studies were overlaid on the simulated profiles.[13,39]

Predicted AUC and C_{max} ratios of digoxin following administration of verapamil were 1.20 (trial range: 1.14–1.28) and 1.19 (range: 1.16–1.23) when the metabolite was considered, and 1.18 (trial range: 1.16–1.20) and 1.17 (range: 1.16–1.20) when the metabolite was not accounted for. It is noteworthy that the upper 95% confidence interval (CI) for the AUC and C_{max} ratios for the individual trials ranged from 1.32 to 1.62 and from 1.27 to 1.47, respectively, which were reasonably consistent with observed values of 1.50 (AUC ratio over 12-h data) and 1.44, respectively. It is also worth noticing that the AUC ratio from $AUC_{(0-\infty)}$ values, as calculated from the graph of *in vivo* data in Rodin et al., can be estimated to be 1.14.

Prediction of the Digoxin–Rifampicin DDI

Predicted and observed mean plasma concentration—time profiles of digoxin after a single oral dose of 1 mg are compared for 10 virtual trials in Figure 3a. Corresponding simulated profiles after administration of rifampicin (600 mg q.d. for 9 days), considering both inhibition and induction of P-gp, are shown in Figure 3b. Predicted and observed mean plasma concentration—time profiles associated with 600 mg rifampicin (q.d.) during 9 days of dosing are compared in Figure 3c. All simulated profiles were reasonably consistent with the observed data.

Predicted decreases in $AUC_{(0-\infty)}$ and C_{max} of digoxin following administration of rifampicin were 1.57- (1.42–1.77) and 1.62-fold (1.53–1.70), respectively. Observed values of 1.4- and 2.2-fold have been reported.[4]

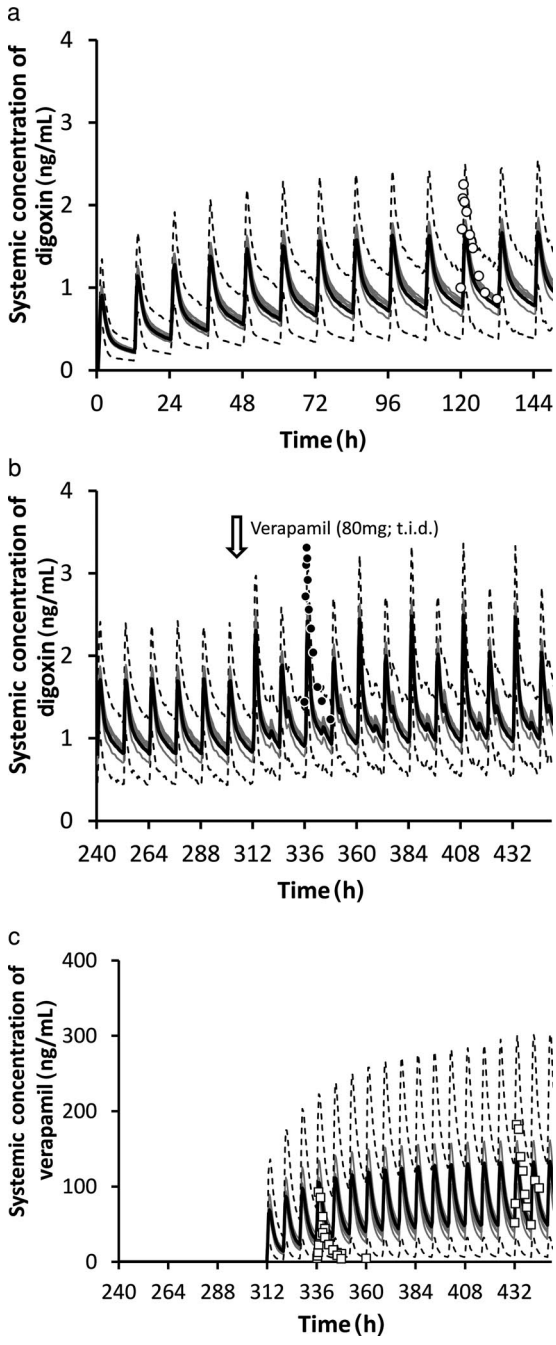

Figure 2. (a) Comparison of observed and predicted plasma concentration–time profiles of digoxin after 0.25 mg oral dose (b.i.d.) for 28 days and (b) for 14 days followed by co-administration of verapamil (80 mg; t.i.d.) for additional 14 days. (c) Concentration–time profiles of verapamil during 80 mg t.i.d. dosing. Key: The thin grey lines represent mean values for individual virtual trials, the thick lines are the overall means of the virtual population ($n = 190$) and the thin black dashed lines are the 95th and 5th percentile of the confidence interval. Open circles—observed digoxin concentrations when administered alone;[37] closed circles—with co-administration of verapamil;[37] open square—observed verapamil concentrations.[13,39]

 DOI 10.1002/jps

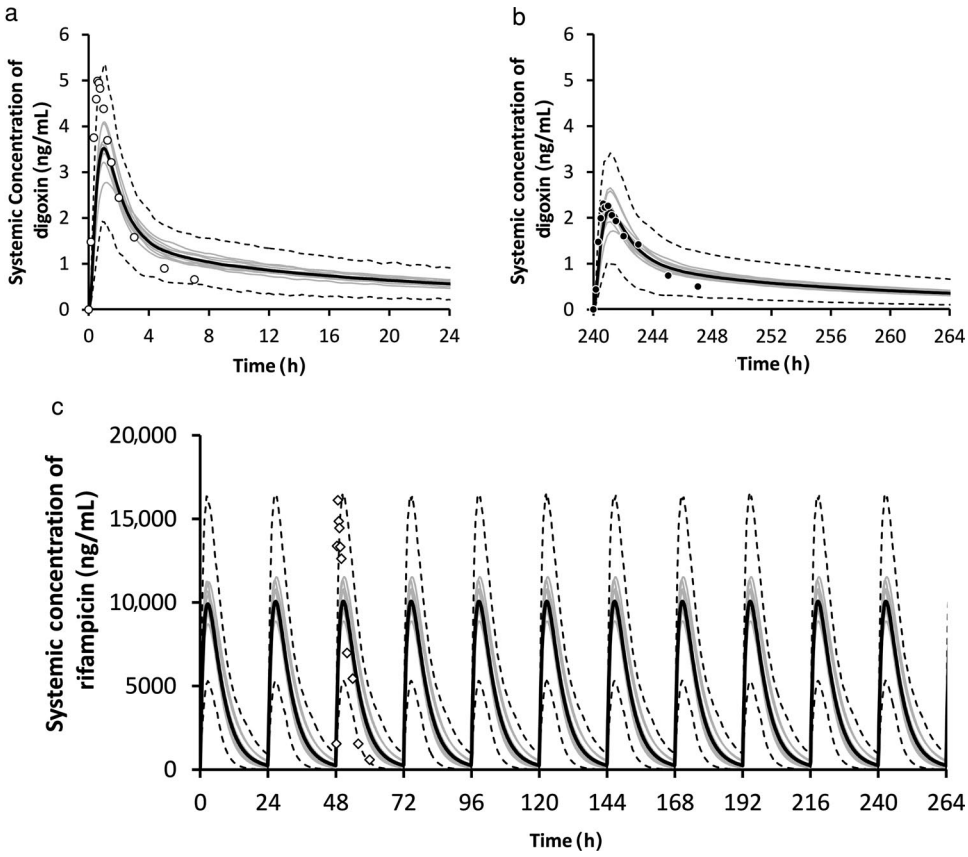

Figure 3. Comparison of observed and predicted plasma concentration–time profiles of digoxin after a single oral dose of 1 mg digoxin (a) on day 1 (i.e., in the absence of rifampicin) and (b) on day 11 after administration of the 11th dose of rifampicin (600 mg, q.d.). Part (C) shows the profiles of rifampicin during 600 mg q.d. dosing. Key: The thin grey lines represent mean values for 10 individual virtual trials, the thick lines are the overall means of the virtual population ($n = 80$) and the dashed black lines are the 95th and 5th percentile of the confidence interval. Open circles—observed digoxin concentrations when administered alone;[4] closed circles—with co-administration of rifampicin;[4] open diamantes—observed rifampicin concentrations.[38]

DISCUSSION

P-glycoprotein has broad substrate specificity and is therefore, susceptible to a range of DDIs with a variety of substrates and inhibitors, including verapamil and its primary metabolite norverpamil.[1,12] However, it should be noted that few of the DDIs, that are clinically relevant, can be attributed solely to the inhibition of P-gp-mediated efflux because of the overlapping substrate specificity between CYP3A4 and P-gp and other confounding factors such as binding replacement from or reduced binding affinity of the Na,K-ATPase.[40] As digoxin is a P-gp substrate and is mainly excreted unchanged via the kidneys, it is an appropriate drug to use for assessment of the P-gp inhibitory potential of drugs in development. In the current study, we have applied the model developed previously for digoxin (Part I) to investigate the inhibitory potential of both verapamil and norverapamil on the P-gp-mediated efflux of digoxin in both gut and liver.

The full PBPK model and the minimal PBPK model that were developed for verapamil and its primary metabolite, respectively, were able to generate plasma concentration–time profiles that were reasonably consistent with observed data (Figs. 1c and 1d). It should be noted that values of CL and V that allowed recovery of observed data were applied for the metabolite. The fact that this model was then able to predict, with reasonable accuracy, the CYP3A4/5-mediated DDI with midazolam provided some confidence that the concentrations of inhibitor simulated within the gut and liver ($Cu_{IW,liver}$) were appropriate for linking *in vitro* information to clinical observations (Fig. 1). Thus, the model was then used to simulate the interaction with digoxin (Fig. 2). Although the mean predicted value for the increase in C_{max} was lower than the observed value (1.19- vs. 1.44-fold), it should be noted that the

upper 95% CI for the C_{max} ratios for the individual trials were 1.27–1.47.

As far as possible, a model should rely upon the most biologically and physiologically plausible assumptions and not solely the recovery of observed data. Thus, though a model may be entirely fit-for-purpose in terms of the original application (drug combination and doses), it may not be applicable to other scenarios. Hence, rival models that produce similar outcomes, despite using varying assumptions, should be contrasted and investigated until an adequate distinction is made through emerging data under varying conditions. When the verapamil metabolite was not accounted for, the simulated C_{max} and AUC ratios were 1.17 and 1.18, respectively. The upper 95% CI for the C_{max} and AUC ratios for the individual trials were 1.25 and 1.34. Inclusion of the metabolite marginally improved variability predictions; hence we decided to keep it as part of the model.

As inputs to the PBPK models, the *in vitro* data require interrogation. The kinetic data for digoxin and inhibition data for verapamil, norverapamil and rifampicin were generated using Caco-2 cell monolayers. The latter were not generated in the same laboratory and therefore, are subject to inter-laboratory variation, which is one of the main contributors to difference in IC_{50} values.[20] In addition, none of the published IC_{50} data were generated via modelling of the *in vitro* data, accounting for the free concentration at the binding site of P-gp; these are apparent IC_{50} values [41] (Table 4). Therefore, the worst-case scenario was simulated using the lowest K_i values calculated from the IC_{50} data.[33]

Despite this, the DDI with digoxin was underpredicted. Further simulations indicate that if the intestinal and hepatic P-gp of digoxin are completely blocked, the predicted AUC and C_{max} ratios for an average individual are 1.6 and 1.83, respectively. Thus, it may be that there are issues with the *in vitro* methods and subsequent analysis used for estimating K_i values for P-gp inhibitors. Alternatively, digoxin is mainly renally cleared and it has been reported that P-gp plays an important role in the kidney. It may be that if inhibition of P-gp-mediated efflux of digoxin in the kidney is accounted for within the PBPK model, then recovery of the observed DDI could be improved. Some clinical studies indicate that the renal clearance of digoxin is reduced following co-administration of verapamil. However, there is conflicting evidence in the literature regarding the contribution of P-gp to the disposition of digoxin in the kidney. Initial simulations (not shown) using the recently developed mechanistic kidney model (Mech KiM) within the Simcyp Simulator[42] indicate that inhibition of renal P-gp-mediated efflux is not propagated directly to the concentration–time profile, but rather to the change in renal mass concentration. Therefore, it would be interesting to extend our PBPK model of digoxin to include P-gp-mediated luminal efflux and tubular secretion of digoxin.

Talinolol is a false-negative case example when the $[I]/IC_{50}$ equation is used to predict a P-gp-mediated DDI.[20] This is possibly related to the involvement of uptake transporters at the basolateral membrane of the gut.[43,44] Static equations are not capable or even meant to handle such scenarios. However, these processes can be adequately described in PBPK models that can provide valuable insights into what is happening inside the cells. Application of correct time-varying concentration at the transporter binding site plays a vital role in obtaining reliable predictions of tDDI when using true values of inhibitory constants.

The model was able to successfully reflect the change in the digoxin concentration–time profile due to induction of intestinal P-gp after rifampicin dosing (600 mg q.d.; 6 days) using an increased REF value (Fig. 3). TDI and induction for metabolising enzymes have already been successfully simulated and these existing models[30] can be modified to address induction or suppression of transporters. However, application of these models to P-gp will require system values related to the turnover of P-gp itself, comparable with those for CYPs,[32] which—to the best of the authors knowledge—are not yet publicly available. Some recent papers highlight the importance of accounting for the time course of P-gp markers.[45] Indeed, induction of intestinal P-gp may be one reason that, for some compounds, the cut-off values of the current P-gp decision tree[16] fail.[18,45] We propose a strategy here for assessing the induction potential of a drug in development. *In vitro* assays can be used to generate P-gp induction data in Caco-2 cells.[46] These can be linked to *in vivo* induction data, which is evaluated using LC–MS/MS absolute abundance measurements[25] or quantitative Western Blot data,[4] following chronic dosing of the drug of interest. This is in effect, what was performed in the current study.

In vitro induction data generated from Caco-2 cells can provide guidance on the inhibitory potential of a drug using cut-off values. If intestinal P-gp induction is observed *in vitro*, a PBPK model may be able to provide more accurate guidance on the tDDI potential of a drug and avoid false positives, that is, drugs with limited tDDI potential that based on the current P-gp decision tree are recommended for *in vivo* tDDI evaluation. It should also be noted that even when the perpetrator has been identified as an inducer of intestinal P-gp, and the predicted decrease in C_{max} and/or AUC for digoxin is found to be negligible *in vivo*, the C_{max} and AUC of the perpetrator itself may be reduced because of the increased expression of functional intestinal P-gp. Further research into the P-gp induction potential of drugs on the market and those in development is warranted. The full PBPK model

described here, that includes a permeability-limited intestinal (ADAM) and liver model (PerL), can be used to estimate the tDDI potential of drugs in complex scenarios involving multiple mechanisms such as inhibition and induction of intestinal or/and hepatic P-gp and other transporters.[45]

CONCLUSION

In conclusion, PBPK models for verapamil and its metabolite, norverapamil, were developed and once validated, used to assess P-gp-mediated DDI with digoxin. Integration of sophisticated permeability-limited models in the gut and liver for digoxin allowed investigation of the inhibition of P-gp-mediated efflux in both organs by verapamil and its metabolite. Thus, it is envisaged that in addition to being a valuable research tool, the approach described here can become effective within drug development programs to reduce the possibility of obtaining false-positive P-gp-mediated DDIs based upon $[I]/IC_{50}$. Although other mechanisms may be involved, the work described here represents a step in the right direction.

As a tool, this model helps to delineate the different factors affecting digoxin pharmacokinetics through simulation. Hence, it can assist with identifying the role of P-gp in absorption and distribution not only for digoxin but also other compounds during drug development. Moreover, unlike static models, it enables assessment of the impact upon the whole plasma profile of digoxin (including C_{max}) and provides measures of inter-individual population variability.

Conflicts of interest: Sibylle Neuhoff, Karen Rowland-Yeo, Zoe Barter, Masoud Jamei and David Turner are employees in Simcyp Limited (a Certara Company). Amin Rostami-Hodjegan is an employee of the University of Manchester and part-time secondee to Simcyp Limited (a Certara Company). Simcyp's research is funded by a consortium of pharmaceutical companies.

ACKNOWLEDGMENTS

This work was funded by Simcyp Limited (a Certara company). The Simcyp Simulator is freely available, following completion of the training workshop, to approved members of academic institutions and other non-for-profit organisations for research and teaching purposes. The help of James Kay and Emma Booker in preparing the manuscript is appreciated.

REFERENCES

1. Fenner KS, Troutman MD, Kempshall S, Cook JA, Ware JA, Smith DA, Lee CA. 2009. Drug-drug interactions mediated through P-glycoprotein: Clinical relevance and in vitro-in vivo correlation using digoxin as a probe drug. Clin Pharmacol Ther 85(2):173–181.
2. Wacher VJ, Wu CY, Benet LZ. 1995. Overlapping substrate specificities and tissue distribution of cytochrome P450 3A and P-glycoprotein: Implications for drug delivery and activity in cancer chemotherapy. Mol Carcinog 13(3):129–134.
3. Wacher VJ, Silverman JA, Zhang Y, Benet LZ. 1998. Role of P-glycoprotein and cytochrome P450 3A in limiting oral absorption of peptides and peptidomimetics. J Pharm Sci 87(11):1322–1330.
4. Greiner B, Eichelbaum M, Fritz P, Kreichgauer HP, von Richter O, Zundler J, Kroemer HK. 1999. The role of intestinal P-glycoprotein in the interaction of digoxin and rifampin. J Clin Invest 104(2):147–153.
5. Ochs HR, Greenblatt DJ, Bodem G, Harmatz JS. 1978. Dose-independent pharmacokinetics of digoxin in humans. Am Heart J 96(4):507–511.
6. Pedersen KE, Dorph-Pedersen A, Hvidt S, Klitgaard NA, Nielsen-Kudsk F. 1981. Digoxin-verapamil interaction. Clin Pharmacol Ther 30(3):311–316.
7. Klein HO, Lang R, Weiss E, Di Segni E, Libhaber C, Guerrero J, Kaplinsky E. 1982. The influence of verapamil on serum digoxin concentration. Circulation 65(5):998–1003.
8. Pedersen KE, Dorph-Pedersen A, Hvidt S, Klitgaard NA, Pedersen KK. 1982. The long-term effect of verapamil on plasma digoxin concentration and renal digoxin clearance in healthy subjects. Eur J Clin Pharmacol 22(2):123–127.
9. Belz GG, Doering W, Munkes R, Matthews J. 1983. Interaction between digoxin and calcium antagonists and antiarrhythmic drugs. Clin Pharmacol Ther 33(4):410–417.
10. Doering W. 1983. Effect of coadministration of verapamil and quinidine on serum digoxin concentration. Eur J Clin Pharmacol 25(4):517–521.
11. Johnson BF, Wilson J, Marwaha R, Hoch K, Johnson J. 1987. The comparative effects of verapamil and a new dihydropyridine calcium channel blocker on digoxin pharmacokinetics. Clin Pharmacol Ther 42(1):66–71.
12. Pauli-Magnus C, von Richter O, Burk O, Ziegler A, Mettang T, Eichelbaum M, Fromm MF. 2000. Characterization of the major metabolites of verapamil as substrates and inhibitors of P-glycoprotein. J Pharmacol Exp Ther 293(2):376–382.
13. McAllister RG, Jr., Kirsten EB. 1982. The pharmacology of verapamil. IV. Kinetic and dynamic effects after single intravenous and oral doses. Clin Pharmacol Ther 31(4):418–426.
14. Park GD, Spector R, Goldberg MJ, Feldman RD. 1987. Digoxin toxicity in patients with high serum digoxin concentrations. Am J Med Sci 294(6):423–428.
15. Piergies AA, Worwag EM, Atkinson AJ, Jr. 1994. A concurrent audit of high digoxin plasma levels. Clin Pharmacol Ther 55(3):353–358.
16. CDER. 2012. Guidance for industry. Drug interaction studies—Study design, data analysis, implications for dosing, and labeling recommendations. Food and Drug Admininstration, US Department of Health and Human Services . http://www.fda.gov/downloads/Drugs/GuidanceComplianceRegulatoryInformation/Guidances/ucm292362.pdf
17. Zhang L, Zhang YD, Strong JM, Reynolds KS, Huang SM. 2008. A regulatory viewpoint on transporter-based drug interactions. Xenobiotica 38(7–8):709–724.
18. Agarwal S, Arya V, Zhang L. 2012. Review of P-gp inhibition data in recently approved new drug applications: Utility of the proposed [I1]/IC50 and [I2]/IC50 criteria in the P-gp decision tree. J Clin Pharmacol 53(2):228–233.
19. Bentz J, O'Connor M, Bednarczyk D, Coleman J, Lee CA, Palm J, Pak YA, Perloff ES, Reyner E, Balimane P, Brännström M, Chu X, Funk C, Guo A, Hanna I, Herédi-Szabó K, Hillgren K, Li L, Hollnack-Pusch E, Jamei M, Lin X, Mason AK, Neuhoff S, Patel A, Podila L, Plise E, Rajaraman GG, Salphati L, Sands E, Taub M, Taur J, Weitz D, Wortelboer HM, Xia C, Xiao G, Yabut Y, Yamagata T, Zhang L, Ellens H. 2013. Variability

in P-glycoprotein inhibitory potency (IC50) using various in vitro experimental systems: Implications for universal digoxin DDI risk assessment decision criteria. Drug Metab Dispos Accepted.
20. Ellens H, Deng S, Coleman J, Bentz J, Taub M, Ragueneau-Majlessi I, Chung SP, Herédi-Szabó K, Neuhoff S, Palm J, Balimane P, Zhang L, Jamei M, Hanna I, O'Connor M, Bednarczyk D, Forsgard M, Chu X, Funk C, Guo A, Hillgren K, Li L, Pak AY, Perloff ES, Rajaraman GG, Salphati L, Taur J, Weitz D, Wortelboer HM, Xia C, Xiao G, Yamagata T, Lee CA. 2013. Application of receiver operating characteristics to refine the prediction of potential digoxin drug interactions. Drug Metab Dispos Accepted.
21. Rowland Yeo K, Jamei M, Rostami-Hodjegan A. 2013. Predicting drug-drug interactions: Application of physiologically based pharmacokinetic models under a system biology approach. Expert Rev Clin Pharmacol 6(2):147–153.
22. Varma MV, Lai Y, Kimoto E, Goosen TC, El-Kattan AF, Kumar V. 2013. Mechanistic modeling to predict the transporter- and enzyme-mediated drug-drug interactions of repaglinide. Pharm Res 30(4):1188–1199.
23. Gertz M, Cartwright CM, Hobbs MJ, Kenworthy KE, Rowland M, Houston JB, Galetin A. 2013. Cyclosporine inhibition of hepatic and intestinal CYP3A4, uptake and efflux transporters: Application of PBPK modeling in the assessment of drug-drug interaction potential. Pharm Res 30(3):761–780.
24. Neuhoff S, Rowland Yeo K, Barter Z, Jamei M, Turner D, Rostami-Hodjegan A. 2013. Application of permeability-limited physiologically-based pharmacokinetic models: Part I—Digoxin pharmacokinetics incorporating P-glycoprotein-mediated efflux. J Pharm Sci Accepted.
25. Harwood MD, Neuhoff S, Carlson GL, Warhurst G, Rostami-Hodjegan A. 2012. Absolute abundance and function of intestinal drug transporters: A prerequisite for fully mechanistic in vitro-in vivo extrapolation of oral drug absorption. Biopharm Drug Dispos 34(1):2–28.
26. Rodgers T, Rowland M. 2007. Mechanistic approaches to volume of distribution predictions: Understanding the processes. Pharm Res 24(5):918–933.
27. Rostami-Hodjegan A, Tucker GT. 2004. 'In silico' simulations to assess the 'in vivo' consequences of 'in vitro' metabolic drug-drug interactions. Drug Discov Today Technol 1(4):441–448.
28. Kroemer HK, Echizen H, Heidemann H, Eichelbaum M. 1992. Predictability of the in vivo metabolism of verapamil from in vitro data: Contribution of individual metabolic pathways and stereoselective aspects. J Pharmacol Exp Ther 260(3):1052–1057.
29. Tracy TS, Korzekwa KR, Gonzalez FJ, Wainer IW. 1999. Cytochrome P450 isoforms involved in metabolism of the enantiomers of verapamil and norverapamil. Br J Clin Pharmacol 47(5):545–552.
30. Rowland Yeo K, Jamei M, Yang J, Tucker GT, Rostami-Hodjegan A. 2010. Physiologically based mechanistic modelling to predict complex drug-drug interactions involving simultaneous competitive and time-dependent enzyme inhibition by parent compound and its metabolite in both liver and gut—The effect of diltiazem on the time-course of exposure to triazolam. Eur J Pharm Sci 39(5):298–309.
31. Rowland Yeo K, Walsky RL, Jamei M, Rostami-Hodjegan A, Tucker GT. 2011. Prediction of time-dependent CYP3A4 drug-drug interactions by physiologically based pharmacokinetic modelling: Impact of inactivation parameters and enzyme turnover. Eur J Pharm Sci 43(3):160–173.
32. Yang J, Liao M, Shou M, Jamei M, Yeo KR, Tucker GT, Rostami-Hodjegan A. 2008. Cytochrome p450 turnover: Regulation of synthesis and degradation, methods for determining rates, and implications for the prediction of drug interactions. Curr Drug Metab 9(5):384–394.
33. Cheng Y, Prusoff WH. 1973. Relationship between the inhibition constant (K1) and the concentration of inhibitor which causes 50 per cent inhibition (I50) of an enzymatic reaction. Biochem Pharmacol 22(23):3099–3108.
34. Jamei M, Marciniak S, Feng K, Barnett A, Tucker G, Rostami-Hodjegan A. 2009. The Simcyp population-based ADME simulator. Expert Opin Drug Metab Toxicol 5(2):211–223.
35. Howgate EM, Rowland Yeo K, Proctor NJ, Tucker GT, Rostami-Hodjegan A. 2006. Prediction of in vivo drug clearance from in vitro data. I: Impact of inter-individual variability. Xenobiotica 36(6):473–497.
36. Backman JT, Olkkola KT, Aranko K, Himberg JJ, Neuvonen PJ. 1994. Dose of midazolam should be reduced during diltiazem and verapamil treatments. Br J Clin Pharmacol 37(3):221–225.
37. Rodin SM, Johnson BF, Wilson J, Ritchie P, Johnson J. 1988. Comparative effects of verapamil and isradipine on steady-state digoxin kinetics. Clin Pharmacol Ther 43(6):668–672.
38. Loos U, Musch E, Jensen JC, Mikus G, Schwabe HK, Eichelbaum M. 1985. Pharmacokinetics of oral and intravenous rifampicin during chronic administration. Klin Wochenschr 63(23):1205–1211.
39. Mattila J, Mantyla R, Taskinen J, Mannisto P. 1985. Pharmacokinetics of sustained-release verapamil after a single administration and at steady state. Eur J Drug Metab Pharmacokinet 10(2):133–138.
40. Ball WJ, Jr., Tse-Eng D, Wallick ET, Bilezikian JP, Schwartz A, Butler VP, Jr. 1981. Effect of quinidine on the digoxin receptor in vitro. J Clin Invest 68(4):1065–1074.
41. Zamek-Gliszczynski MJ, Lee CA, Poirier A, Bentz J, Chu X, Ellens H, Ishikawa T, Jamei M, Kalvass JC, Nagar S, Pang KS, Korzekwa K, Swaan PW, Taub ME, Zhao P, Galetin A. 2013. ITC recommendations on transporter kinetic parameter estimation and translational modeling of transport-mediated PK and DDIs in humans. Clin Pharmacol Ther Accepted.
42. Neuhoff S, Gaohua L, Burt H, Jamei M, Li L, Tucker GT, Rostami-Hodjegan A. In Press. Accounting for transporters in renal clearance: Towards a mechanistic kidney model (Mech KiM). In Transporters in drug discovery, development and use; Steffansen B, Sugiyama Y, Eds. New York: Springer.(In press)
43. Oswald S, Terhaag B, Siegmund W. 2011. In vivo probes of drug transport: Commonly used probe drugs to assess function of intestinal P-glycoprotein (ABCB1) in humans. Handb Exp Pharmacol (201):403–447.
44. Shirasaka Y, Mori T, Shichiri M, Nakanishi T, Tamai I. 2012. Functional pleiotropy of organic anion transporting polypeptide OATP2B1 due to multiple binding sites. Drug Metab Pharmacokinet 27(3):360–364.
45. Fukushima K, Kobuchi S, Mizuhara K, Aoyama H, Takada K, Sugioka N. Time-dependent interaction of ritonavir in chronic use: The power balance between inhibition and induction of P-glycoprotein and cytochrome P450 3A. J Pharm Sci In Press.
46. Anderle P, Niederer E, Rubas W, Hilgendorf C, Spahn-Langguth H, Wunderli-Allenspach H, Merkle HP, Langguth P. 1998. P-Glycoprotein (P-gp) mediated efflux in Caco-2 cell monolayers: The influence of culturing conditions and drug exposure on P-gp expression levels. J Pharm Sci 87(6):757–762.
47. Keefe DL, Yee YG, Kates RE. 1981. Verapamil protein binding in patients and in normal subjects. Clin Pharmacol Ther 29(1):21–26.
48. Robinson MA, Mehvar R. 1996. Enantioselective distribution of verapamil and norverapamil into human and rat erythrocytes: The role of plasma protein binding. Biopharm Drug Dispos 17(7):577–587.
49. Hansch C, Leo A, Hoekman D. 1995. Exploring QSAR: Hydrophobic, electronic, and steric constants. Washington, DC: American Chemical Society.

50. Tannergren C. 2004. Intestinal permeability and presystemic extraction of fexofenadine and R/S-verapamil. Comprehensive Summaries of Uppsala Dissertations from the Faculty of Pharmacy. Faculty of Pharmacy, Uppsala University. p 53.
51. Engman H, Tannergren C, Artursson P, Lennernas H. 2003. Enantioselective transport and CYP3A4-mediated metabolism of R/S-verapamil in Caco-2 cell monolayers. Eur J Pharm Sci 19(1):57–65.
52. Neuhoff S, Artursson P, Zamora I, Ungell AL. 2006. Impact of extracellular protein binding on passive and active drug transport across Caco-2 cells. Pharm Res 23(2):350–359.
53. Eichelbaum M, Mikus G, Vogelgesang B. 1984. Pharmacokinetics of (+)-, (-)- and (+/-)-verapamil after intravenous administration. Br J Clin Pharmacol 17(4):453–458.
54. Woodcock BG, Rietbrock I, Vohringer HF, Rietbrock N. 1981. Verapamil disposition in liver disease and intensive-care patients: Kinetics, clearance, and apparent blood flow relationships. Clin Pharmacol Ther 29(1):27–34.
55. Johnston A, Burgess CD, Hamer J. 1981. Systemic availability of oral verapamil and effect on PR interval in man. Br J Clin Pharmacol 12(3):397–400.
56. Schomerus M, Spiegelhalder B, Stieren B, Eichelbaum M. 1976. Physiological disposition of verapamil in man. Cardiovasc Res 10(5):605–612.
57. Dilger K, Eckhardt K, Hofmann U, Kucher K, Mikus G, Eichelbaum M. 1999. Chronopharmacology of intravenous and oral modified release verapamil. Br J Clin Pharmacol 47(4):413–419.
58. Wagner CC, Simpson M, Zeitlinger M, Bauer M, Karch R, Abrahim A, Feurstein T, Schutz M, Kletter K, Muller M, Lappin G, Langer O. 2011. A combined accelerator mass spectrometry-positron emission tomography human microdose study with 14C- and 11C-labelled verapamil. Clin Pharmacokinet 50(2):111–120.
59. Ho PC, Ghose K, Saville D, Wanwimolruk S. 2000. Effect of grapefruit juice on pharmacokinetics and pharmacodynamics of verapamil enantiomers in healthy volunteers. Eur J Clin Pharmacol 56(9–10):693–698.
60. Kimura Y, Kioka N, Kato H, Matsuo M, Ueda K. 2007. Modulation of drug-stimulated ATPase activity of human MDR1/P-glycoprotein by cholesterol. Biochem J 401(2):597–605.
61. Troutman MD, Thakker DR. 2003. Novel experimental parameters to quantify the modulation of absorptive and secretory transport of compounds by P-glycoprotein in cell culture models of intestinal epithelium. Pharm Res 20(8):1210–1224.
62. Ohashi R, Tamai I, Nezu Ji J, Nikaido H, Hashimoto N, Oku A, Sai Y, Shimane M, Tsuji A. 2001. Molecular and physiological evidence for multifunctionality of carnitine/organic cation transporter OCTN2. Mol Pharmacol 59(2):358–366.
63. Yong CL, Kunka RL, Bates TR. 1980. Factors affecting the plasma protein binding of verapamil and norverapamil in man. Res Commun Chem Pathol Pharmacol 30(2):329–339.
64. Czejka MJ, Zwoelfer N, Podesser B. 1992. Red blood cell partitioning of gallopamil, verapamil and norverapamil. Farmaco 47(3):387–391.
65. Sigma–Aldrich. 2013. A case study in SPE method development—Understanding the dual interaction properties of discovery DSC-SCX SPE using verapamil (and metabolite) from serum as a TEST example. Reporter EU 10.
66. Eichelbaum M, Ende M, Remberg G, Schomerus M, Dengler HJ. 1979. The metabolism of DL-[14C]verapamil in man. Drug Metab Dispos 7(3):145–148.
67. Burman WJ, Gallicano K, Peloquin C. 2001. Comparative pharmacokinetics and pharmacodynamics of the rifamycin antibacterials. Clin Pharmacokinet 40(5):327–341.
68. Drusano GL, Townsend RJ, Walsh TJ, Forrest A, Antal EJ, Standiford HC. 1986. Steady-state serum pharmacokinetics of novobiocin and rifampin alone and in combination. Antimicrob Agents Chemother 30(1):42–45.
69. Polk RE, Brophy DF, Israel DS, Patron R, Sadler BM, Chittick GE, Symonds WT, Lou Y, Kristoff D, Stein DS. 2001. Pharmacokinetic interaction between amprenavir and rifabutin or rifampin in healthy males. Antimicrob Agents Chemother 45(2):502–508.
70. Kajosaari LI, Laitila J, Neuvonen PJ, Backman JT. 2005. Metabolism of repaglinide by CYP2C8 and CYP3A4 in vitro: Effect of fibrates and rifampicin. Basic Clin Pharmacol Toxicol 97(4):249–256.
71. Acocella G, Pagani V, Marchetti M, Baroni GC, Nicolis FB. 1971. Kinetic studies on rifampicin. I. Serum concentration analysis in subjects treated with different oral doses over a period of two weeks. Chemotherapy 16(6):356–370.
72. Tran JQ, Kovacs SJ, McIntosh TS, Davis HM, Martin DE. 1999. Morning spot and 24-hour urinary 6 beta-hydroxycortisol to cortisol ratios: Intraindividual variability and correlation under basal conditions and conditions of CYP 3A4 induction. J Clin Pharmacol 39(5):487–494.
73. Choo EF, Leake B, Wandel C, Imamura H, Wood AJ, Wilkinson GR, Kim RB. 2000. Pharmacological inhibition of P-glycoprotein transport enhances the distribution of HIV-1 protease inhibitors into brain and testes. Drug Metab Dispos 28(6):655–660.
74. Ekins S, Kim RB, Leake BF, Dantzig AH, Schuetz EG, Lan LB, Yasuda K, Shepard RL, Winter MA, Schuetz JD, Wikel JH, Wrighton SA. 2002. Three-dimensional quantitative structure-activity relationships of inhibitors of P-glycoprotein. Mol Pharmacol 61(5):964–973.
75. Elsby R, Surry DD, Smith VN, Gray AJ. 2008. Validation and application of Caco-2 assays for the in vitro evaluation of development candidate drugs as substrates or inhibitors of P-glycoprotein to support regulatory submissions. Xenobiotica 38(7–8):1140–1164.
76. Kawahara I, Kato Y, Suzuki H, Achira M, Ito K, Crespi CL, Sugiyama Y. 2000. Selective inhibition of human cytochrome P450 3A4 by N-[2(R)-hydroxy-1(S)-indanyl]-5-[2(S)-(1, 1-dimethylethylaminocarbonyl)-4-[(furo[2, 3-b]pyridin-5-yl)methyl]piperazin-1-yl]-4(S)-hydroxy-2(R)-phenylmethy lpentanamide and P-glycoprotein by valspodar in gene transfectant systems. Drug Metab Dispos 28(10):1238–1243.
77. Tang F, Horie K, Borchardt RT. 2002. Are MDCK cells transfected with the human MDR1 gene a good model of the human intestinal mucosa? Pharm Res 19(6):765–772.